Multiple short-range contributions to the $0\nu\beta\beta$ decay process for probing beyond the Standard Model

Altay Etkin* and Frank F. Deppisch†
Department of Physics and Astronomy, University College London, Gower Street, London WC1E 6BT, United Kingdom
(Dated: September 29, 2022)

Neutrinoless double beta decay is a crucial test for lepton number violation in particle physics. Observation of this process would have fundamental implications for neutrino physics, theories beyond the Standard Model and cosmology. Within this mindset, using the IBM-2 framework and previously achieved constraints between single short-ranged contributions at a time as well as between standard light neutrino mass and with one short-range contribution leading to interference among them, we extend the work to multi-contributions without assuming any form of restriction on the parameter space. It is shown that such contributions are achieved upon constructing effective normalised couplings written in a 3×3 symmetric and real matrix, for which bounds on the quadratic form defined by the neutrinoless double-beta decay inverse half-life formula, leads to ellipsoid constraints on these effective parameters.

I. INTRODUCTION

While the Standard Model (SM) explains very accurately the interactions observed during high-energy experiments, the spontaneous symmetry breaking of the gauge group $SU(3) \times SU(2) \times U(1)$ yields masses to the charged fermions via the Higgs mechanism. Albeit this explains why charged fermions do have mass, neutrinos seems to evade from this mechanism, as only left-handed neutrinos have been detected so far. This puts neutrinos to a special position, as they cannot acquire a Dirac mass, as most charged fermions of the SM do. It is also well known that neutrinos due possess a small mass and can oscillate between generations, known as neutrino oscillation. In order to incorporate this tiny neutrino mass within the SM, it would either require the presence of sterile neutrino states which would assume that neutrinos are Majorana particles, namely their antiparticle and particle states coincide; or effective lepton number violating interactions (LNV). Concerning the first scenario, the generation of Dirac neutrino masses analogous to those of the charged fermions are allowed, this nevertheless requires very small Higgs-Yukawa couplings and that the total lepton number will no longer be an accidental symmetry as the sterile neutrinos would acquire a LNV Majorana mass. The seesaw mechanism is among scenarios where sterile neutrinos do exist and possess Majorana masses of order 10^{14} GeV with light neutrino masses of order 0.1 eV [1]. The seesaw mechanism is also one among scenarios where the lepton number is violated. These type of models are not the only scenarios generating light-neutrino masses: there also exists the possibility to include LNV interactions at low scales, higher loop orders and higher-dimensional effective interactions. Such lepton number breaking occurring close to the electroweak scale would force higher-dimensional LNV operators to be taken seriously into account. We here focus on the search for $0\nu\beta\beta$ decay as the most sensitive approach to probe Majorana neutrino masses and explore possibilities for beyond the SM physics (BSM).

Currently, the lower limit on the neutrinoless double-beta decay half-life is set by the Germanium isotope $^{76}_{32}$Ge [1, 2]

$$T_{1/2}(^{76}_{32}\mathrm{Ge}) > 1.8 \times 10^{26} \text{ yr}. \tag{1}$$

There exist two possible mechanisms for $0\nu\beta\beta$ decay. The first one is the so-called long-range transitions via exchange of a light neutrino which includes the standard mass mechanism, where the exchanged neutrinos are Majorana. This mass mechanism is sensitive to the effective neutrino mass $m_{\beta\beta} := \sum_i U_{ei}^2 m_{\nu_i}$, where the sum is over light Majorana neutrino masses and U_{ei} is the charged-current leptonic mixing matrix elements. One can calculate the inverse decay half-life given an isotope by

$$T_{1/2}^{-1} := \left(\underbrace{\frac{|m_{\beta\beta}|}{m_e}}_{|\epsilon_\nu|} \right)^2 G_\nu |M_\nu|^2, \tag{2}$$

with the phase space factor (PSF) G_ν and the nuclear matrix element (NME) M_ν. The dimensionless parameter ϵ_ν is made of the electron mass and the light Majorana neutrino mass, which is taken to be very small. With the bound in Eq. (1) the limit set on the effective neutrino mass is $|m_{\beta\beta}| \leq 79-180$ meV at 90% confidence level for an unquenced axial coupling $g_A = 1.27$ [2] and with the uncertainty due to the NMEs arising from different nuclear models. This mass mechanism creates a dim-5 operator. However, in BSM scenarios, the insertion of a neutrino mass is not necessarily a requirement. For such a case, we talk about dim-7 operators, where SM vertices in the $0\nu\beta\beta$ decay Feynman diagram are replaced with effective operator vertices. However, due to

* altay.etkin.19@ucl.ac.uk; Also at Department of Physics, Imperial College London, London UK
† f.deppisch@ucl.ac.uk

the neutrino helicity-flip intrinsic in the operator, typical mechanisms are suppressed by the light neutrino masses. It is difficult to have a dim-7 operator with exotic long-range contributions dominating over the standard mass mechanism [3, 4], although it can be achieved in UV-complete theories with a modestly suppressed standard contribution [5–8]. The second mechanism is the more complicated short-range contributions where all mediating particles are heavier than 100 Mev and represented as contact interactions with six external fermions. This process probes LNV physics around the TeV scale. A similar expression to Eq. (2) is given by

$$T_{1/2}^{-1} := |\epsilon_I|^2 G_I |M_I|^2. \tag{3}$$

Albeit such light-neutrino exchanges are not involved with short-range contributions, lepton number breaking and Majorana type SM neutrinos are required. The short-range and standard mass mechanisms are thus expected to compete but the relative strength is highly dependent on the underlying model.

In previous papers [1, 4], NMEs and PSFs have been calculated according to the interacting boson model (IBM-2) framework. Using them will allow to set upper limits on the effective short-range couplings ϵ_I and look for various interference effects between standard light-neutrino exchange and short-range mechanisms.

The paper is organised as follows. In Section II we start by reviewing the short-range effective lepton number violating interactions Lagrangian density and various neutrino mass models available throughout the literature. We then move in Section III in reviewing the calculations for the NMEs and PSFs using previous work [1] and data provided by the IBM-2 framework. Using the decay inverse half-life, we put in Section IV numerical constraints on single coupling contributions, in the presence of interference between light neutrino and short-range mechanisms and finally we deal with multiple contributions with interference terms by considering a 3×3 matrix model. Section V concludes our discussion with a summary and an outlook.

II. SHORT-RANGE EFFECTIVE LNV LAGRANGIAN AND NEUTRINO MASS MODELS

In this work, we start by reviewing short-range effective LNV operators that are considered within the $0\nu\beta\beta$ decay process and then look at the various potential interplay with standard mass mechanisms.

A. LNV effective Lagrangian for short-range contributions

The LNV effective Lagrangian for short-range contributions consists of five different Lorentz-invariant fermion current products summed over different chiralities, namely

$$\mathcal{L}_{SR} := \frac{G_F^2 cos^2\theta_C}{2m_p} \sum_{C_1,C_2,c} \Big(\epsilon_1^{C_1,C_2,c} J_{C_1} J_{C_2} j_c + \epsilon_2^{C_1,C_2,c} J_{C_1}^{\mu\nu} J_{\mu\nu,C_2} j_c + \epsilon_3^{C_1,C_2,c} J_{C_1}^{\mu} J_{\mu,C_2} j_c + \epsilon_4^{C_1,C_2,c} J_{C_1}^{\mu} J_{\mu\nu,C_2} j^{\nu} + \epsilon_5^{C_1,C_2,c} J_{C_1}^{\mu} J_{C_2} j_{\mu} \Big) \tag{4}$$

The effective operators are given by:

$$\begin{aligned} \mathcal{O}_{\mathrm{R/L}} &\equiv \mathcal{O}_{\mathrm{S\pm P}} := 1 \pm \gamma_5, \\ \mathcal{O}^{\mu}_{\mathrm{R/L}} &\equiv \mathcal{O}^{\mu}_{\mathrm{V\pm A}} := \gamma^{\mu}\mathcal{O}_{\mathrm{S\pm P}}, \\ \mathcal{O}^{\mu\nu}_{\mathrm{R/L}} &\equiv \mathcal{O}^{\mu\nu}_{\mathrm{T_{L/R}}} := \sigma^{\mu\nu}\mathcal{O}_{\mathrm{T_{L/R}}}, \end{aligned}$$

where $\sigma^{\mu\nu} = \frac{i}{1}[\gamma^{\mu}, \gamma^{\nu}]$. The corresponding effective hadronic and leptonic currents given in Eq. (4) are respectively

$$\begin{aligned} J_{\mathrm{R/L}} &\equiv J_{\mathrm{S\pm P}} := \overline{u}^a \mathcal{O}_{\mathrm{R/L}} d_a, \\ J^{\mu}_{\mathrm{R/L}} &\equiv J^{\mu}_{\mathrm{V\pm A}} := \overline{u}^a \mathcal{O}^{\mu}_{\mathrm{R/L}} d_a, \\ J^{\mu\nu}_{\mathrm{R/L}} &\equiv J^{\mu\nu}_{\mathrm{T_{R/L}}} := \overline{u}^a \mathcal{O}^{\mu\nu}_{\mathrm{R/L}} d_a, \\ j_{\mathrm{R/L}} &\equiv j_{\mathrm{S\pm P}} := \overline{e} \mathcal{O}_{\mathrm{R/L}} e^c, \\ j^{\mu} &:= \overline{e}\gamma^{\mu}\gamma_5 e^c, \end{aligned}$$

with $e^c = Ce$ the charge conjugation operator. With these nine-dimensional operators, one can construct the corresponding twenty-four basis components all invariant

under the gauge group $SU(3)_{\rm C} \times U(1)_{\rm Q}$:

$$\begin{aligned}
\epsilon_1^{RRR} &\sim J_{\rm R} J_{\rm R} j_{\rm R}, \\
\epsilon_1^{RRL} &\sim J_{\rm R} J_{\rm R} j_{\rm L}, \\
\epsilon_1^{LRR} \equiv \epsilon_1^{RLR} &\sim J_{\rm L} J_{\rm R} j_{\rm R}, \\
\epsilon_1^{LRL} \equiv \epsilon_1^{RLL} &\sim J_{\rm L} J_{\rm R} j_{\rm L}, \\
\epsilon_1^{LLR} &\sim J_{\rm L} J_{\rm L} j_{\rm R}, \\
\epsilon_1^{LLL} &\sim J_{\rm L} J_{\rm L} j_{\rm L}, \\
\epsilon_2^{RRR} &\sim J_{\rm R}^{\mu\nu} J_{\mu\nu,{\rm R}} j_{\rm R}, \\
\epsilon_2^{RRL} &\sim J_{\rm R}^{\mu\nu} J_{\mu\nu,{\rm R}} j_{\rm L}, \\
\epsilon_2^{LLR} &\sim J_{\rm L}^{\mu\nu} J_{\mu\nu,{\rm L}} j_{\rm R}, \\
\epsilon_2^{LLL} &\sim J_{\rm L}^{\mu\nu} J_{\mu\nu,{\rm L}} j_{\rm L}, \\
\epsilon_3^{RRR} &\sim J_{\rm R}^{\mu} J_{\mu,{\rm R}} j_{\rm R}, \\
\epsilon_3^{RRL} &\sim J_{\rm R}^{\mu} J_{\mu,{\rm R}} j_{\rm L}, \\
\epsilon_3^{LRR} \equiv \epsilon_3^{RLR} &\sim J_{\rm L}^{\mu} J_{\mu,{\rm R}} j_{\rm R}, \\
\epsilon_3^{LRL} \equiv \epsilon_3^{RLL} &\sim J_{\rm L}^{\mu} J_{\mu,{\rm R}} j_{\rm L}, \\
\epsilon_3^{LLR} &\sim J_{\rm L}^{\mu} J_{\mu,{\rm L}} j_{\rm R}, \\
\epsilon_3^{LLL} &\sim J_{\rm L}^{\mu} J_{\mu,{\rm L}} j_{\rm L}, \\
\epsilon_4^{RR} &\sim J_{\rm R}^{\mu} J_{\mu\nu,{\rm R}} j^{\nu}, \\
\epsilon^{RL}4 &\sim J_{\rm R}^{\mu} J_{\mu\nu,{\rm L}} j^{\nu}, \\
\epsilon_4^{LR} &\sim J_{\rm L}^{\mu} J_{\mu\nu,{\rm R}} j^{\nu}, \\
\epsilon_4^{LL} &\sim J_{\rm L}^{\mu} J_{\mu\nu,{\rm L}} j^{\nu}, \\
\epsilon_5^{RR} &\sim J_{\rm R}^{\mu} J_{\rm R} j_{\nu}, \\
\epsilon_5^{RL} &\sim J_{\rm R}^{\mu} J_{\rm L} j_{\nu}, \\
\epsilon_5^{LR} &\sim J_{\rm L}^{\mu} J_{\rm R} j_{\nu}, \\
\epsilon_5^{LL} &\sim J_{\rm L}^{\mu} J_{\rm L} j_{\nu}.
\end{aligned}$$

All other terms are identically zero due to particular identities and the Pauli exclusion principle.

B. New physics scenarios with short-range mechanisms

Concerning the leading explanation for the $0\nu\beta\beta$ decay, the exchange of light Majorana neutrinos are to be considered. However, being a long-ranged mechanism, it arises from a different Lagrangian than that of Eq. (4) [1]. This gives rise to the mass mechanism sensitive to the effective Majorana neutrino mass, namely

$$m_{\beta\beta} = \sum_{i=1}^{3} U_{ei}^2 m_{\nu_i}, \tag{5}$$

which leads to the half-life decay formula given by Eq. (2). To extend such a contribution would be to include sterile fermionic states under the SM gauge interactions which acquires mass without spoiling the SM gauge invariance and mix with the SM neutrinos after electroweak symmetry breaking. In fact, for sterile neutrinos much lighter than the nuclear physics scale, their contributions are analogous to that the previous approach. An interesting scenario arises if the Majorana states are in charge for the light neutrino masses in a seesaw mechanism, in which both contributions cancel out. On the other hand, for sterile neutrinos much heavier than the nuclear physics scale, they can be integrated out which results in a contribution involving the operators $\mathcal{O}_{\rm L}^{\mu}\mathcal{O}_{{\rm L},\mu}\mathcal{O}_{\rm L}$ with coupling ϵ_3^{LLL} given by

$$\epsilon_3^{LLL} = \sum_{i=1}^{n_N} V_{eN_i}^2 \frac{m_p}{m_{N_i}}. \tag{6}$$

One could also look for non-trivial extensions of the SM, such as the minimal left-right symmetric model (LRSM) which is based on the gauge group $SU(3)_{\rm C} \times SU(2)_L \times SU(2)_R \times U(1)_{\rm B\text{-}L}$. This model contains as a requirement right-handed Majorana neutrinos, forming a doublet together with the right-handed leptons, where the charged currents are being mediated via a right-handed W-boson. The LRSM gauge group is understood to be spontaneously broken to that of the SM at a high scale giving masses to the right-handed W-boson and Majorana neutrinos. The SM neutrino acquire masses through mixing with the heavy neutrinos and the vacuum expectation value of an electroweak triplet Higgs scalar. The above mentioned trivial mechanisms are thus apparent features of the LRSM. In addition, contributions from a heavy neutrino and two right-handed W-bosons gives rise to short-ranged operators with coupling ϵ_3^{RRR} given by

$$\epsilon_3^{RRR} = \left(\frac{g_R^2}{g^2}\frac{\cos(\theta_C^R)}{\cos(\theta_C)}\frac{m_W^2}{m_{W_R}^2}\right)^2 \sum_{i=1}^{3} (U_{ei}^R)^2 \frac{m_p}{m_{N_i}}. \tag{7}$$

Another important contribution comes from the mixing of the W and W_R bosons which leads to couplings

$$\begin{aligned}
\epsilon_3^{LRR} &= \sin(\theta_{LR}^W)\frac{g}{g_R}\frac{\cos(\theta_C)}{\cos(\theta_C^R)}\frac{m_{W_R}^2}{m_W^2}\epsilon_3^{RRR}, \\
\epsilon_3^{LLR} &= \sin^2(\theta_{LR}^W)\left(\frac{g}{g_R}\frac{\cos(\theta_C)}{\cos(\theta_C^R)}\frac{m_{W_R}^2}{m_W^2}\right)^2 \epsilon_3^{RRR}.
\end{aligned} \tag{8}$$

All other type 3 contributions are cancelled out by mixing between the light-heavy neutrinos and large W_R boson masses. Finally, the last contribution is like mentioned above due to the electroweak triplet Higgs scalars with couplings analogous to Eq. (7-8).

III. NUCLEAR MATRIX ELEMENTS AND PHASE SPACE FACTORS

The NMEs for short-range mechanisms have been analytically derived in [1, 4]. We follow the approach therein.

A. Nuclear form factors and their corresponding NMEs

The form factors with their corresponding parametrizations and charges are given by

$$\begin{aligned}
F_S(q^2) &= \frac{g_S}{(1+q^2/m_V^2)^2},\\
F_{P'}(q^2) &= \frac{g_{P'}}{(1+q^2/m_V^2)^2}\frac{1}{1+q^2/m_\pi^2},\\
F_V(q^2) &= \frac{g_V}{(1+q^2/m_V^2)^2},\\
F_W(q^2) &= \frac{g_W}{(1+q^2/m_V^2)^2},\\
F_A(q^2) &= \frac{g_A}{(1+q^2/m_V^2)^2},\\
F_P(q^2) &= \frac{g_P}{(1+q^2/m_V^2)^2}\frac{1}{1+q^2/m_\pi^2},\\
F_{T_i}(q^2) &= \frac{g_{T_i}}{(1+q^2/m_V^2)^2},
\end{aligned} \tag{9}$$

with $g_S = g_V = 1.0$, $g_{P'} = 349$, $g_W = 3.7$, $g_A = 1.269$, $g_P = 231$ and $g_{T_i} = 1.0, -3.3, 1.34$, respectively; and with shape parameters given by $m_V = 0.84$ GeV, $m_A = 1.09$ GeV and the pion mass $m_\pi = 138$ MeV. The form factors $F_V(q^2)$, $F_W(q^2)$ and $F_A(q^2)$ are determined experimentally and the parametrizations above provide a decent description below 200 MeV. On the other hand, as it is not possible to directly obtain the induced pseudo-scalar form factor from experiment, we use the parametrization suggested in [9], which is based on the partially conserved axial-vector current hypothesis.

The NMEs for the five short-range operators will generally depend on the chiralities of the two quark currents involved. These are

$$\begin{aligned}
\mathcal{M}_1 &:= g_S^2\mathcal{M}_F \pm \frac{g_{P'}^2}{12}(M_{\rm GT}^{'P'P'} + M_{\rm T}^{'P'P'}),\\
\mathcal{M}_2 &:= -2g_{T_1}^2\mathcal{M}_{\rm GT}^{T_1T_1},\\
\mathcal{M}_3 &:= g_V^2\mathcal{M}_F \pm \frac{(g_V+g_W)^2}{12}(-2M_{\rm GT}^{'AP} + M_{\rm T}^{'WW})\\
&\quad \mp\Big[g_A^2\mathcal{M}_{\rm GT}^{AA} - \frac{g_Ag_P}{6}(\mathcal{M}_{\rm GT}^{'AP} + \mathcal{M}_T^{'AP})\\
&\quad + \frac{g_P^2}{48}(\mathcal{M}_{\rm GT}^{''AP} + \mathcal{M}_T^{''PP})\Big],\\
\mathcal{M}_4 &:= \mp i\Big[g_Ag_{T_1}\mathcal{M}_{\rm GT}^{AT_1} - \frac{g_Pg_{T1}}{12}(\mathcal{M}_{\rm GT}^{'PT_1} + \mathcal{M}_{\rm T}^{'PT_1})\Big],\\
\mathcal{M}_5 &:= g_Vg_S\mathcal{M}_F \pm \Big[\frac{g_Ag_{P'}}{12}(\tilde{\mathcal{M}}_{\rm GT}^{AP'} + \tilde{\mathcal{M}}_{\rm T}^{AP'})\\
&\quad - \frac{g_Pg_{P'}}{24}(\mathcal{M}_{\rm GT}^{'q_0PP'} + \mathcal{M}_{\rm T}^{'q_0PP'})\Big].
\end{aligned} \tag{10}$$

In addition, we also consider the standard light neutrino exchange mechanism with the NME given as

$$\begin{aligned}
\mathcal{M}_\nu &:= g_V^2\mathcal{M}_F - g_A^2\mathcal{M}_{\rm GT}^{AA} + \frac{g_Ag_P}{6}(\mathcal{M}_{\rm GT}^{'AP} + \mathcal{M}_T^{'AP})\\
&\quad + \frac{(g_V+g_W)^2}{12}(-2\mathcal{M}_{\rm GT}^{-WW} + \mathcal{M}_T^{'WW})\\
&\quad - \frac{g_P^2}{48}(\mathcal{M}_{\rm GT}^{''PP} + \mathcal{M}_T^{''PP}).
\end{aligned} \tag{11}$$

In order to evaluate Eqs. (10-11), we use the numerical values of the NMEs calculated within the IBM-2 model for various isotopes are given according to Table I for the first five $\mathcal{M}_i$ and Table II for the standard light neutrino exchange.

The corresponding compound NMEs $\mathcal{M}_1$ to $\mathcal{M}_5$ according to the IBM-2 model and the values given in Table I and Table II are given in Table III. They are listed for all distinct combinations of quark chiralities and calculated using the quenched value $g_A = 1.0$.

B. Leptonic PSFs and decay rates

Now that the NMEs are known, we have to also consider decay rates for the neutrinoless double-beta decay. This is achieved via the calculation of the so-called leptonic phase space factors. The numerical results are followed from [1]. The leptonic matrix elements are given by

$$\begin{aligned}
f_{11\pm}^{(0)} &:= \pm|f^{-1-1}|^2 \pm |f_11|^2 + |f_1^{-1}|^2 + |f_1^{-1}|^2,\\
f_{11\pm}^{(1)} &:= -2(f_1^{-1}f_1^{-1} \pm f^{-1-1}f_{11}),\\
f_{66}^{(0)} &:= 16(|f^{-1-1}|^2 + |f_{11}|^2),\\
f_{66}^{(1)} &:= 32f^{-1-1}f_{11},\\
f_{16}^{(0)} &:= 4(|f_{11}|^2 - |f^{-1-1}|^2),\\
f_{16}^{(1)} &:= 0.
\end{aligned} \tag{12}$$

With the NMEs calculated in the previous subsection and the values of the squared leptonic matrix elements given in Eq. (12), the full differential rate of $0^+ \to 0^+0\nu\beta\beta$ is expressed as

$$\frac{d^2\Gamma}{dE_1 d\cos\theta} := Cw(E_1)(a(E_1 + b(E_1)\cos\theta)), \tag{13}$$

where C is a constant given in terms of the SM Fermi coupling, Cabibbo angle and electrons mass; and $w(E_1) = E_1E_2p_1p_2$. The coefficients $a(E_1)$ and $b(E_2)$ are more involved, namely

TABLE I: NMEs for short-range neutrinoless double-beta decay mechanisms evaluated in the IBM-2.

Isotope	$\mathcal{M}_F$	$\mathcal{M}^{AA}_{\rm GT}$	$\mathcal{M}^{AT_1}_{\rm GT}$	$\mathcal{M}^{T_1T_1}_{\rm GT}$	$\mathcal{M}^{'WW}_{\rm GT}$	$\mathcal{M}^{'WW}_{\rm T}$	$\mathcal{M}^{'AP}_{\rm GT}$	$\mathcal{M}^{'AP}_{\rm T}$	$\mathcal{M}^{'PT_1}_{\rm GT}$	$\mathcal{M}^{'PT_1}_{\rm T}$	$\mathcal{M}^{'P'P'}_{\rm GT}$	$\mathcal{M}^{'P'P'}_{\rm T}$	$\mathcal{M}^{''PP}_{\rm GT}$	$\mathcal{M}^{''PP}_{\rm T}$
^{76}Ge	-48.89	170.0	174.3	173.5	2.945	6.541	2.110	1.310	2.255	1.183	0.798	0.271	0.028	0.022
^{82}Se	41.22	140.7	144.3	143.6	2.456	6.206	1.758	1.249	1.878	1.183	0.660	0.259	0.024	0.021
^{100}Mo	51.96	181.9	188.1	188.6	4.590	8.055	2.273	1.590	2.464	1.128	0.910	0.317	0.029	0.027
^{110}Pd	43.52	151.2	156.5	157.0	3.945	6.816	1.892	1.356	2.055	1.223	0.762	0.271	0.024	0.023
^{124}Sn	33.19	104.2	106.7	106.1	1.701	3.655	1.321	0.723	1.407	0.651	0.489	0.146	0.018	0.012
^{134}Xe	39.45	124.7	127.8	127.2	2.111	4.191	1.564	0.823	1.669	0.741	0.585	0.163	0.021	0.014

TABLE II: NMEs for the standard light neutrino exchange neutrinoless double-beta decay mechanism evaluated in the IBM-2.

Isotope	$\mathcal{M}_F$	$\mathcal{M}^{AA}_{\rm GT}$	$\mathcal{M}^{'AP}_{\rm GT}$	$\mathcal{M}^{'AP}_{\rm T}$	$\mathcal{M}^{'WW}_{\rm GT}$	$\mathcal{M}^{'WW}_{\rm T}$	$\mathcal{M}^{''PP}_{\rm GT}$	$\mathcal{M}^{''PP}_{\rm T}$
^{76}Ge	0.780	6.062	0.036	0.010	0.089	0.035	3.4×10^4	1.4×10^4
^{82}Se	0.667	4.928	0.030	0.010	0.073	0.034	4.1×10^4	1.3×10^4
^{100}Mo	0.511	5.553	0.038	0.012	0.096	0.041	4.7×10^4	1.6×10^4
^{110}Pd	0.425	4.432	0.032	0.009	0.080	0.036	3.9×10^4	1.4×10^4
^{124}Sn	0.572	3.370	0.021	0.005	0.053	0.018	2.5×10^4	7.5×10^5
^{134}Xe	0.686	4.211	0.026	0.005	0.064	0.023	3.0×10^4	8.3×10^5

$$
\begin{aligned}
a(E_1) \quad &:= f^{(0)}_{11+}\left|\sum_{i=1}^{3}\epsilon^L_i\mathcal{M}_i+\frac{m_{\beta\beta}}{m_e}\mathcal{M}_\nu\right|^2+f^{(0)}_{11+}\left|\sum_{i=1}^{3}\epsilon^R_i\mathcal{M}_i\right|^2+\frac{f^{(0)}_{66}}{16}\left|\sum_{i=4}^{5}\epsilon_i\mathcal{M}_i\right|^2\\
&+f^{(0)}_{11-}\times 2{\rm Re}\left[\left(\sum_{i=1}^{3}\epsilon^L_i\mathcal{M}_i+\frac{m_{\beta\beta}}{m_e}\mathcal{M}_\nu\right)\left(\sum_{i=1}^{3}\epsilon^R_i\mathcal{M}_i\right)^*\right]\\
&+\frac{f^{(0)}_{16}}{4}\times 2{\rm Re}\left[\left(\sum_{i=1}^{3}\epsilon^L_i\mathcal{M}_i+\frac{m_{\beta\beta}}{m_e}\mathcal{M}_\nu-\sum_{i=1}^{3}\epsilon^R_i\mathcal{M}_i\right)\left(\sum_{i=4}^{5}\epsilon_i\mathcal{M}_i\right)^*\right] \qquad (14)\\
b(E_1) \quad &:= f^{(1)}_{11+}\left|\sum_{i=1}^{3}\epsilon^L_i\mathcal{M}_i+\frac{m_{\beta\beta}}{m_e}\mathcal{M}_\nu\right|^2+f^{(1)}_{11+}\left|\sum_{i=1}^{3}\epsilon^R_i\mathcal{M}_i\right|^2+\frac{f^{(0)}_{66}}{16}\left|\sum_{i=4}^{5}\epsilon_i\mathcal{M}_i\right|^2. \qquad (15)
\end{aligned}
$$

These expressions are valid under the presence of any combination of short-range mechanisms and the NMEs are defined over the different short-range current types 1 through 5 including different chiralities. One should also keep in mind that a distinction is made for the short-range mechanism ranging from 1 to 3 as the scalar current is either left-handed or right-handed, indicated by the chirality notation R/L. This distinction represents the interference behaviour between terms of different electron chiralities. For instance, the first term on the right-hand side of Eq. (14) describes the contributions of and interference among the short range mechanisms ranging from 1 to 3 with left-handed electron chiralities and that of the light-neutrino mechanism. All other terms are understood in a similar fashion.

Despite the completeness of the fully differential decay rate given by Eq. (13) which contains the complete kinematic information and integration over the whole electron phase space will yield the total rate, of experimental interest are the distribution over the single-electron energy and the angular correlation. The single electron energy distribution is simply given by

$$\frac{d\Gamma}{dE_1} := 2Cw(E_1)a(E_1), \qquad (16)$$

and the angular distribution reads

$$\frac{d\Gamma}{d\cos\theta} := \frac{\Gamma}{2}(1+K\cos\theta), \qquad (17)$$

where

$$K := \frac{\int_{m_e}^{Q_{\beta\beta}+m_e} dE_1 w(E_1)b(E_1)}{\int_{m_e}^{Q_{\beta\beta}+m_e} dE_1 w(E_1)a(E_1)}. \qquad (18)$$

One can also integrate the total differential rate over the whole electron phase space to determine the total decay rate and the decay half-life. This results in the total decay rate being given by

$$\Gamma = \frac{\ln 2}{T_{1/2}}, \qquad (19)$$

TABLE III: Compound NMEs for all distinct quark current chirality combinations, calculated using the quenched value $g_A = 1.0$.

Isotope	$\mathcal{M}_1^{XX}$	$\mathcal{M}_1^{XY}$	$\mathcal{M}_2^{XX}$	$\mathcal{M}_3^{Xx}$	$\mathcal{M}_3^{XY}$	$\mathcal{M}_4^{XX}$	$\mathcal{M}_5^{XX}$	$\mathcal{M}_5^{XY}$	$\mathcal{M}_\nu$
^{76}Ge	5300	−5400	−174	−200	99.8	−158	202	−301	-6.64
^{82}Se	4030	-4110	-144	-171	83.3	-134	114	-199	-5.46
^{100}Mo	12400	-12500	-189	124	83.9	134	1230	-1340	-5.27
^{110}Pd	10400	-10500	-157	-102	69.3	-107	1030	-1120	-4.21
^{124}Sn	3450	-3520	-106	-124	56.2	-95.3	157	-224	-3.79
^{134}Xe	4240	-4320	-127	-146	67.6	-114	196	-277	-4.67

where the inverse half-life is given by

$$\begin{aligned} T_{1/2}^{-1} &:= G_{11+}^{(0)} \left| \sum_{i=1}^{3} \epsilon_i^L \mathcal{M}_i + \frac{m_{\beta\beta}}{m_e} \mathcal{M}_\nu \right|^2 + G_{11+}^{(0)} \left| \sum_{i=1}^{3} \epsilon_i^R \mathcal{M}_i \right|^2 + G_{66}^{(0)} \left| \sum_{i=4}^{5} \epsilon_i \mathcal{M}_i \right|^2 \\ &+ G_{11-}^{(0)} \times 2\mathrm{Re}\left[\left(\sum_{i=1}^{3} \epsilon_i^L \mathcal{M}_i + \frac{m_{\beta\beta}}{m_e} \mathcal{M}_\nu \right) \left(\sum_{i=1}^{3} \epsilon_i^R \mathcal{M}_i \right)^* \right] \\ &+ G_{16}^{(0)} \times 2\mathrm{Re}\left[\left(\sum_{i=1}^{3} \epsilon_i^L \mathcal{M}_i + \frac{m_{\beta\beta}}{m_e} \mathcal{M}_\nu - \sum_{i=1}^{3} \epsilon_i^R \mathcal{M}_i \right) \left(\sum_{i=4}^{5} \epsilon_i \mathcal{M}_i \right)^* \right]. \end{aligned} \tag{20}$$

The coefficients $G_{IJ}^{(0)}$ are the integrated PSFs defined by [1]

$$\begin{aligned} G_{IJ}^{(0,1)} &:= \frac{2C g_{IJ}^{(0,1)}}{4\ln 2 R_A^2} \int_{m_e}^{Q_{\beta\beta}+m_e} dE_1 w(E_1) \\ &\times f_{IJ}^{(0,1)}(E_1, Q_{\beta\beta} + 2m_e - E_1), \end{aligned} \tag{21}$$

where $g_{11\pm}^{(0,1)} = 1$, $g_{66}^{(0,1)} = 1/16$ and $g_{16}^{(0,1)} = 1/4$. These integrated PSFs for the different isotopes we considered are given in Table IV.

TABLE IV: Integrated PSFs used in calculating the total decay rate for the light neutrino and short-range mechanisms.

Isotope	$G_{11+}^{(0)}$	$G_{11-}^{(0)}$	$G_{66}^{(0)}$	$G_{16}^{(0)}$	$G_{11}^{(1)}$	$G_{66}^{(1)}$
			$[10^{-15}$ yr$^{-1}]$			
^{76}Ge	2.360	-0.280	1.320	0.870	-1.954	0.977
^{82}Se	10.19	-0.712	5.450	2.925	-9.079	4.539
^{100}Mo	15.91	-1.053	8.482	4.456	-14.25	7.125
^{110}Pd	4.807	-0.541	2.674	1.730	-4.014	2.007
^{124}Sn	9.028	-0.843	4.935	2.976	-7.760	3.880
^{134}Xe	0.597	-0.164	0.380	0.323	-0.394	0.197

IV. NUMERICAL RESULTS

With the NMEs and integrated PSFs defined in the previous section, we can now construct numerical bounds on the short-ranged couplings and effective neutrino mass.

A. Numerical bounds on single-coupling contributions

For the case of the effective neutrino mass, with $\epsilon_\nu = m_{\beta\beta}/m_e$ and all other couplings set identically to zero, the inverse half-life formula simplifies to

$$T_{1/2}^{-1} = G_{11+}^{(0)} \left(\frac{|m_{\beta\beta}|}{m_e} |\mathcal{M}_\nu| \right)^2. \tag{22}$$

Likewise, assuming one short-ranged coupling at a time and setting everything else, including light neutrino coupling identically to zero leads to

$$T_{1/2}^{-1} = G_i^{(0)} |\epsilon_i \mathcal{M}_i|^2. \tag{23}$$

The numerical values for upper limits on the effective neutrinoless double-beta decay mass and short-range couplings are given in Table V with the resulting limits at 90% confidence level.

TABLE V: Upper limits on the effective mass and the short-range couplings from current experimental bounds $T_{1/2}^{\rm exp}$ at 90% C.L., assuming a single contribution at a time and $g_A = 1.0$. These also include quark chirality combinations.

Isotope	$T_{1/2}^{\rm exp}[yr]$	$\lvert m_{\beta\beta}\rvert$ [meV]	$\lvert\epsilon_1^{XX}\rvert$	$\lvert\epsilon_1^{XY}\rvert$	$\lvert\epsilon_2^{XX}\rvert$ $[10^{-10}]$	$\lvert\epsilon_3^{XX}\rvert$	$\lvert\epsilon_3^{XY}\rvert$	$\lvert\epsilon_4\rvert$	$\lvert\epsilon_5^{XX}\rvert$	$\lvert\epsilon_5^{XY}\rvert$
^{76}Ge	1.8×10^{26}	118	2.90	2.84	88.4	77.1	154	130	102	68.1
^{82}Se	2.4×10^{24}	599	15.9	15.5	445	375	768	654	764	440
^{100}Mo	1.1×10^{24}	733	6.10	6.04	401	608	901	774	84.1	77.5

B. Numerical bounds in the presence of interference between light neutrino and short-range mechanisms

In the previous subsection, we looked at the different single contributions at a time, i.e. we obtained numerical bounds upon considering one mechanism (which corresponds to a single operator) at a time. We would like to expand this to many contributions which results in interference terms. A large number of possibilities are plausible to investigate, but what we really need is the combination of at least the light neutrino with any other mechanism is expected to show at all levels. This is due to the fact that any new physics scenario with a short-ranged operator is expected to generate Majorana neutrino masses at a level to explain neutrino oscillation.

The first scenario of interest is the interference between light neutrino exchange and the short-range operator ϵ_3^{LLL}. We have seen in Section II B that such an operator is being set off by heavy sterile neutrinos. In such a case, the decay inverse half-life given by Eq. (20) is

$$T_{1/2}^{-1} = G_{11+}^{(0)} \left| \frac{m_{\beta\beta}}{m_e} \mathcal{M}_\nu + \epsilon_3^{LLL} \mathcal{M}_3^{LLL} \right|^2 . \tag{24}$$

Since light neutrino exchange and the operator associated with the short-range coupling given above have the same leptonic structure, the two contributions add coherently. The same observation is made for any left-handed leptonic current associated to $\epsilon_{1,2,3}$. Taking the physical parameters to be real as they should be, and using the fact that the NMEs above are all negative, one can have destructive interference for ϵ_3^{LLL} real and negative, and constructive interference for ϵ_3^{LLL} real and positive, where $m_{\beta\beta}$ is always taken to be positive. The general constraints on both couplings are depicted within Fig. 1a.

In the case of the interference between the standard light neutrino contribution with the coupling ϵ_5^{RR}, the overlap is suppressed by the interference between the different lepton currents involved. In that case, Eq. (20) reads

$$\begin{aligned} T_{1/2}^{-1} &= G_{11+}^{(0)} \frac{|m_{\beta\beta}|^2}{m_e^2} \left|\mathcal{M}_\nu\right|^2 + G_{66}^{(0)} \left|\epsilon_5^{RR}\right|^2 \left|\mathcal{M}_5^{RR}\right|^2 \\ &\quad + 2G_{16}^{(0)} \mathrm{Re}\left[\left(\frac{m_{\beta\beta}}{m_e^2} \mathcal{M}_\nu \right) \left(\epsilon_5^{RR} \mathcal{M}_5^{RR} \right)^* \right] \\ &= A \left|m_{\beta\beta}\right|^2 + B |\epsilon_5^{RR}|^2 + 2C |m_{\beta\beta}| |\epsilon_5^{RR}| \cos(\alpha - \beta), \end{aligned} \tag{25}$$

where $A = G_{11+}^{(0)} \left|\mathcal{M}_\nu\right|^2 / m_e^2$, $B = G_{66}^{(0)} \left|\mathcal{M}_5^{RR}\right|^2$ and $C = G_{16}^{(0)} \left|\mathcal{M}_\nu\right| \left|\mathcal{M}_5^{RR}\right| / m_e$ are positive coefficients such that all coefficients are taken to real numbers. The angle $\alpha - \beta$ is the relative complex phase between $m_{\beta\beta}$ and ϵ_5^{RR}, which is taken to be 0 or π, so that we get a quadratic polynomial in $m_{\beta\beta}$ and ϵ_5^{RR}. With such a polynomial being constrained by the inverse half-life decay, one gets elliptical shapes with the tilting determined by the size of $G_{16}^{(0)}$ relative to $G_{11+}^{(0)}$ and $G_{66}^{(0)}$. These elliptic shapes are given in Fig. 1b for the 76-Germanium and 100-Molybdenum isotopes with two different half-life precision for each.

C. Numerical bounds in the presence of non-trivial interference between all couplings

We have discussed in subsections IV A and IV B that there can be single contributions with no interaction between different couplings, but also interference between two couplings, which for inverse half-lives being polynomials in those couplings could lead to elliptical shapes, with the tildes being determined by the PSFs. We would like to continue towards that path by including not just two but all the couplings. This process being too complicated, we propose to reduce the problem by writing the inverse-half life formula given in Eq. (20) in matrix form. The reason for doing this is related to the fact that interference terms describes geometrically conic sections, as seen from the previous subsection. The generalisation of these sections would involve the theory of matrix representation of conic sections, which combines the tools of linear algebra and that of geometry into one. For our purpose, this construction can be achieved by defining a set of vectors corresponding to each coupling which span a vector space formed by these couplings. However, this can be further simplified by defining various normalised

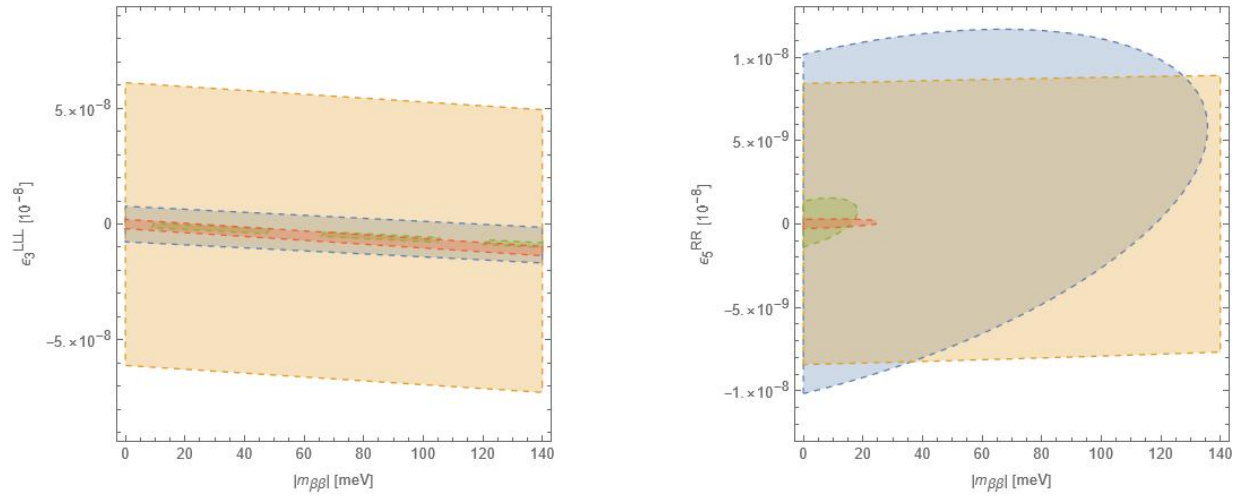

(a) Constraints on the effective $0\nu\beta\beta$ decay mass $|m_{\beta\beta}|$ and the short-range operators coupling ϵ_3^{LLL}

(b) Constraints on the effective $0\nu\beta\beta$ decay mass $|m_{\beta\beta}|$ and the short-range operators coupling ϵ_5^{RR}

FIG. 1: All other couplings are set identically to zero. The highlighted regions denote the allowed parameter space from the current limit on the decay half-life for different isotopes. The blue and green regions are for inverse half-lives for ^{76}Ge with bounds $(1.8\times10^{26})^{-1}$ yr^{-}1 and $(1.1\times10^{28})^{-1}$ yr^{-}1, respectively, whereas the orange and red regions are for inverse half-lives for ^{100}Mo with bounds $(1.1\times10^{24})^{-1}$ yr^{-}1 and $(1.0\times10^{27})^{-1}$ yr^{-}1, respectively.

effective couplings, which are three in total, thus bringing the dimensionality of the problem to three dimension. We are thus expecting to deal with quadratic surfaces such as the three dimensional ellipsoid. Such effective couplings are defined as follows:

$$\begin{aligned}
\epsilon^{L,\nu}_{1\to3} &:= \frac{1}{\mathcal{M}^{L,\nu}_{1\to3}}\left(\sum_{i=1}^{3}\epsilon^{L}_{i}\mathcal{M}_i + \frac{m_{\beta\beta}}{m_e}\mathcal{M}_\nu\right),\\
\epsilon^{R}_{1\to3} &:= \frac{1}{\mathcal{M}^{R}_{1\to3}}\times\sum_{i=1}^{3}\epsilon^{R}_{i}\mathcal{M}_i,\\
\epsilon^{L,R}_{4\to5} &:= \frac{1}{\mathcal{M}^{L,R}_{4\to5}}\times\sum_{i=4}^{5}\epsilon_{i}\mathcal{M}_i.
\end{aligned} \tag{26}$$

Here, the three normalisations factors are given in terms of effective NMEs given by

$$\begin{aligned}
\mathcal{M}^{R}_{1\to3} &:= \sqrt{\sum_{i=1}^{3}\mathcal{M}_i^2},\\
\mathcal{M}^{L,\nu}_{1\to3} &:= \sqrt{\left(\mathcal{M}^{R}_{1\to3}\right)^2+\mathcal{M}_\nu^2},\\
\mathcal{M}^{L,R}_{4\to5} &:= \sqrt{\sum_{i=4}^{5}\mathcal{M}_i^2}.
\end{aligned} \tag{27}$$

One can see that the averages $\mathcal{M}^{R}_{1\to3}$ and $\mathcal{M}^{L,\nu}_{1\to3}$ being related upon the neutrino NME term, $\mathcal{M}^{L,\nu}_{1\to3}$ must be greater than $\mathcal{M}^{R}_{1\to3}$. This would result in the strength of contribution of $\epsilon^{L,\nu}_{1\to3}$ being much stronger than that of the contribution due to $\epsilon^{R}_{1\to3}$.

Assuming that everything is real and together with the three effective couplings defined above, the decay inverse half-life equation can be brought to the following polynomial equation of degree two and with three variables

$$\begin{aligned}
T^{-1}_{1/2} &:= G^{(0)}_{11+}\left(\mathcal{M}^{L,\nu}_{1\to3}\right)^2\left(\epsilon^{L,\nu}_{1\to3}\right)^2\\
&+G^{(0)}_{11+}\left(\mathcal{M}^{R}_{1\to3}\right)^2\left(\epsilon^{R}_{1\to3}\right)^2\\
&+G^{(0)}_{66}\left(\mathcal{M}^{L,R}_{4\to5}\right)^2\left(\epsilon^{L,R}_{4\to5}\right)^2\\
&+2G^{(0)}_{11-}\mathcal{M}^{L,\nu}_{1\to3}\mathcal{M}^{R}_{1\to3}\epsilon^{L,\nu}_{1\to3}\epsilon^{R}_{1\to3}\\
&+2G^{(0)}_{16}\mathcal{M}^{L,\nu}_{1\to3}\mathcal{M}^{L,R}_{4\to5}\epsilon^{L,\nu}_{1\to3}\epsilon^{L,R}_{4\to5}\\
&-2G^{(0)}_{16}\mathcal{M}^{R}_{1\to3}\mathcal{M}^{L,R}_{4\to5}\epsilon^{R}_{1\to3}\epsilon^{L,R}_{4\to5}.
\end{aligned} \tag{28}$$

As can be seen from this equation, the first three terms are independent of each other, leading to single contributions for the effective couplings. The last three terms being cross-terms give rise to various interference terms between the couplings $\epsilon^{L,\nu}_{1\to3}$, $\epsilon^{R}_{1\to3}$ and $\epsilon^{L,R}_{4\to5}$. These terms mix-up non-trivially each of these couplings, as indicated by the matrix form given by Eq. (29). Notice that each element of the matrix are purely in terms of the PSFs and effective NMEs. In addition, the effective NMEs all being defined as square roots makes them positive real numbers. The PSFs being both negative and positive real numbers, they will carry the information about the shape and orientation of the ellipsoids. In fact, bringing

Eq. (28) in matrix form will help us understand better these various shapes. The quadratic form corresponding to the inverse half-life for the $0\nu\beta\beta$ decay reads:

$$T_{1/2}^{-1} = \begin{pmatrix} \epsilon_{1\to3}^{L,\nu} \\ \epsilon_{1\to3}^{R} \\ \epsilon_{4\to5}^{L,R} \end{pmatrix}^T \begin{pmatrix} G_{11+}^{(0)}\left(\mathcal{M}_{1\to3}^{L,\nu}\right)^2 & G_{11-}^{(0)}\mathcal{M}_{1\to3}^{L,\nu}\mathcal{M}_{1\to3}^{R} & G_{16}^{(0)}\mathcal{M}_{1\to3}^{L,\nu}\mathcal{M}_{4\to5}^{L,R} \\ G_{11-}^{(0)}\mathcal{M}_{1\to3}^{L,\nu}\mathcal{M}_{1\to3}^{R} & G_{11+}^{(0)}\left(\mathcal{M}_{1\to3}^{R}\right)^2 & -G_{16}^{(0)}\mathcal{M}_{1\to3}^{R}\mathcal{M}_{4\to5}^{L,R} \\ G_{16}^{(0)}\mathcal{M}_{1\to3}^{L,\nu}\mathcal{M}_{4\to5}^{L,R} & -G_{16}^{(0)}\mathcal{M}_{1\to3}^{R}\mathcal{M}_{4\to5}^{L,R} & G_{66}^{(0)}\left(\mathcal{M}_{4\to5}^{L,R}\right)^2 \end{pmatrix} \begin{pmatrix} \epsilon_{1\to3}^{L,\nu} \\ \epsilon_{1\to3}^{R} \\ \epsilon_{4\to5}^{L,R} \end{pmatrix}. \tag{29}$$

The matrix equation given by Eq. (29) is written in terms of homogeneous coordinates, here represented by the effective couplings. These are coordinates on the projective space of couplings such that the coordinates of points, including points at infinity, can be represented using finite coordinates. The (not most) general equation for a quadratic section in homogeneous coordinates (x, y, z) can be written as

$$Ax^2 + By^2 + Cz^2 + 2Dxy + 2Exz + 2Fyz + G = 0, \tag{30}$$

where the matrix equation of this quadric then takes the simple form

$$\begin{pmatrix} x \\ y \\ z \end{pmatrix}^T \begin{pmatrix} A & D & E \\ D & B & F \\ E & F & C \end{pmatrix} \begin{pmatrix} x \\ y \\ z \end{pmatrix} + G = 0. \tag{31}$$

Thinking of this equation in terms of Eq. (29), we do not yet know whether we have ellipsoids, just like we have ellipses in our interference expression given through Eq. (25). This can be achieved by constructing a diagonal matrix through finding the eigenvalues and eigenvectors of this matrix. First looking at our matrix, we see that it is symmetric, i.e. by the spectral theorem, it has real eigenvalues and is thus orthogonally diagonalizable. Calculating the eigenvalues of this matrix gives:

$$\begin{aligned} \lambda_1 &= 1.52 \times 10^{-7}\ \text{yr}^{-1} \\ \lambda_2 &= 1.19 \times 10^{-7}\ \text{yr}^{-1} \\ \lambda_3 &= 1.17 \times 10^{-10}\ \text{yr}^{-1}. \end{aligned} \tag{32}$$

The associated normalised eigenvectors are

$$v_1 = \begin{pmatrix} 0.71 \\ -0.71 \\ 0.02 \end{pmatrix} \quad v_2 = \begin{pmatrix} 0.71 \\ 0.71 \\ -4.40 \times 10^{-8} \end{pmatrix} \quad v_3 = \begin{pmatrix} -0.02 \\ 0.02 \\ 1.00 \end{pmatrix} \tag{33}$$

We therefore can rewrite the inverse half-life in terms of the sum of eigenvalues multiplied by these new effective couplings squared, namely

$$\begin{aligned} T_{1/2}^{-1} &= \lambda_1\epsilon_{\text{eff},1}^2 + \lambda_2\epsilon_{\text{eff},2}^2 + \lambda_3\epsilon_{\text{eff},3}^2 \\ &= 1.52 \times 10^{-7}\left(0.71\epsilon_{1\to3}^{L,\nu} - 0.71\epsilon_{1\to3}^{R} + 0.02\epsilon_{4\to5}^{L,R}\right)^2 \\ &+1.19 \times 10^{-7}\left(0.71\epsilon_{1\to3}^{L,\nu} + 0.71\epsilon_{1\to3}^{R} - 4.40 \times 10^{-8}\epsilon_{4\to5}^{L,R}\right)^2 \\ &+1.17 \times 10^{-10}\left(-0.02\epsilon_{1\to3}^{L,\nu} + 0.02\epsilon_{1\to3}^{R} + \epsilon_{4\to5}^{L,R}\right)^2. \end{aligned} \tag{34}$$

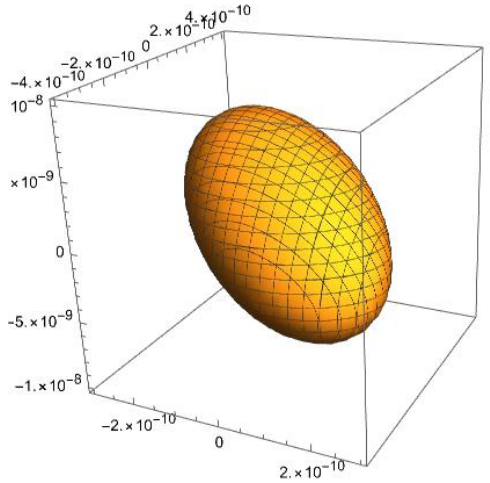

FIG. 2: Ellipsoidal constraint on the effective couplings for ^{76}Ge isotope with inverse half-life bounded to be $(1.8 \times 10^{26})^{-1}$ yr^{-}1.

As noted, this quadratic form does not contain any cross-terms of the form $\epsilon_{\text{eff},i}\epsilon_{\text{eff},j}$. Notice that all terms have the positive sign which indicates that a section of the quadratic surface in the plane $\epsilon_{\text{eff},i} = 0$ for any $i \in 1, 2, 3$, is an ellipse with semi-axes given by the square roots of the eigenvalues. These are depicted in Fig. 3 for the ^{76}Ge and ^{100}Mo isotopes with two decay half-life bounds.The positive signature of all three eigenvalues also indicate that we have an ellipsoid. This is depicted in Fig. 2.

As one can see, the values for the couplings are bounded

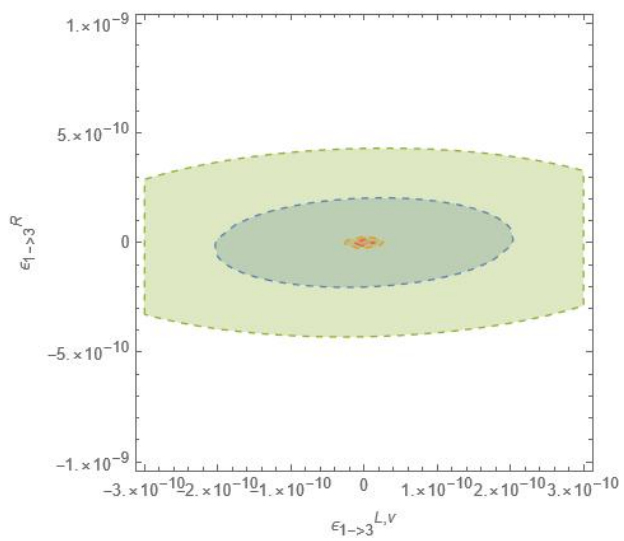

(a) Constraints on $\epsilon^{L,\nu}_{1\to3}$ and $\epsilon^{R}_{1\to3}$.

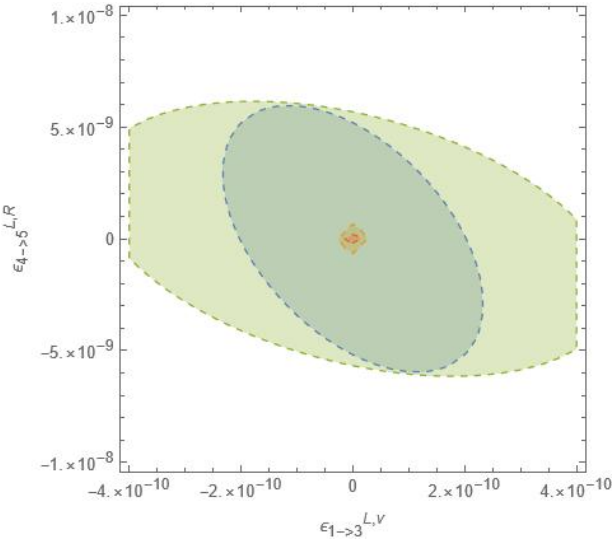

(b) Constraints on $\epsilon^{L,\nu}_{1\to3}$ and $\epsilon^{L,R}_{4\to5}$.

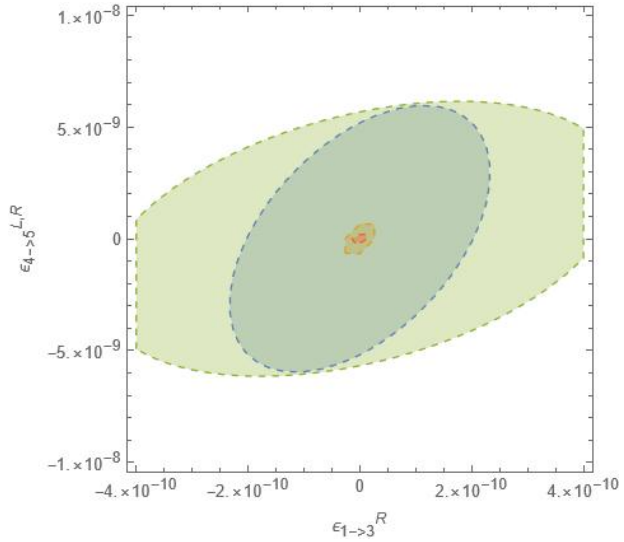

(c) Constraints on $\epsilon^{R}_{1\to3}$ and $\epsilon^{L,R}_{4\to5}$.

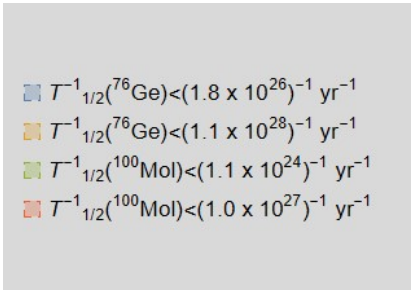

(d)

FIG. 3: These constraints are to be interpreted as cross-sections of the ellipsoid described by the effective couplings $\epsilon_{\text{eff},i}$.

to specific values, namely are allowed to exist within the boundary and interior of the ellipsoid. Just like the previous models, we have constraints due to interference terms between each effective coupling. From the plots, we see that the effective couplings $\epsilon^{L,\nu}_{1\to3}$ and $\epsilon^{R}_{1\to3}$ rotates the ellipse by 45^o degrees and $\epsilon^{L,R}_{4\to5}$ stretches it. It can also be seen that the elliptic section formed by $\epsilon^{L,\nu}_{1\to3}$ and $\epsilon^{R}_{1\to3}$ are tilted by $G^{(0)}_{11+}$ relative to $G^{(0)}_{11-}$.

As discussed above, the eigenvalues are very important not just to discuss about the shapes of the constraints, but as well as the sensitivity. Upon looking at the first two eigenvalues λ_1 and λ_2, they are of the same order of magnitude but differ by their multiplicative factors. The third eigenvalue λ_3 is way smaller than the two other eigenvalues. We know that the higher the sensitivity, the larger the PSFs are to be expected, and hence a larger matrix. We thus want to probe small values of couplings, i.e. λ_3 being very small means the sensitivity in $\epsilon^{L,R}_{4\to5}$ is not very good, whereas for the other two being of the same order of magnitude, can both be sensitive, yet one can choose the first one to be the most sensitive, which means that $\epsilon^{L,\nu}_{1\to3}$ and $\epsilon^{R}_{1\to3}$ are going to be very sensitive.

V. SUMMARY AND CONCLUSION

An understanding of the origin of neutrino masses might be observed through signatures of total lepton

number violation, which is a key open issue in particle physics. Neutrinoless double-beta decay has so far been the only practical means to probe light Majorana neutrino masses at scales indicated by neutrino oscillations. In addition it is sensitive to new physics contributions from exotic particles and interactions coupling to first-generation quarks and electrons. Within an effective field theoretic framework, neutrinoless double-beta decay searches strongly constrain contributions of that form. Within this paper, we looked at short-range contributions which result from integrating out exotic particles much heavier than the energy scale $m_F \approx 100$ MeV of double beta decay, leading to effective dimension-nine operators which is in total twenty-four. Additionally, we use the updated calculations for the standard light neutrino exchange mechanism in [1] to analyse its interaction with short-range contributions.

Using the first complete numerical evaluation of the PSFs and NMEs needed for the description of short-range mechanisms of neutrinoless double-beta decay within the framework of IBM-2 with restoration of the isospin properties of the Fermi transition operator given in [1], we estimated numerical constraints on single and multi-contributions to couplings, given bounds on the decay inverse half-life for various isotopes. These numerical constraints seem to indicate elliptic shapes in the presence of interference terms. Considering one operator at a time, the current limits correspond to operator scales ranging between 3 to 10 TeV, where the strongest sensitivity is achieved for operators enhanced by pion-mediated corrections, in agreement with previous analyses [7, 10–12], in our case arising from enhanced pseudoscalar form factors.

We also looked at multiple couplings all contributing at the same time. In that case, by rewriting the inverse half-life equation as a 3×3 real and symmetric matrix, the quadric surfaces are to be that of an ellipsoid, with its conic sections being elliptical. This is in agreement with our previous standard light-neutrino and one short-range coupling constraint shapes, which were also elliptical. The shapes are highly being affected by the PSFs sign, and the magnitude of the effective NMEs. In fact, this method is very broadly applicable as it can be used to calculate the volume of these different ellipsoids for various isotopes and hence identify the best constraining isotope with the largest volume. Another possibility is to apply the algorithmic setting we developed in this paper to construct a similar approach for long-range contributions to the neutrinoless double-beta decay. This would result in higher dimensional matrices, hence higher dimensional ellipsoids, but the idea should carry on. This is a work left to be done in the future.

These constraints on the effective neutrino mass, short-range operator couplings as well as the normalised effective couplings can be interpreted in terms of new physics scenarios. For instance, in the sterile neutrino case, the most stringent limit as indicated in Table V on $0\nu\beta\beta$ decay contributions of heavy sterile neutrinos is set in ^{136}Xe which means that

$$\left(\sum_{i=1}^{n_N} \frac{V_{eN_i}^2}{m_{N_i}}\right)^{-1} > 1.3 \times 10^8 \text{GeV},$$

assuming contributions from the light Standard Model neutrinos are negligible. This can then be compared with other searches which rules out portions of theoretically allowed values. This method can then be extended to other BSM models and compared with the parameter spaces. A very plausible scenario would be to use the constraints put on the effective operator couplings discussed in this paper to rule out not allowed parameter spaces coming from searches, left to be explored within future papers.

Searches for LNV signatures, with neutrinoless double-beta decay as the most prominent example, are essential in understanding neutrinos and BSM physics. With no clear sign of new physics been observed to the writing of this paper, short-range operators as those considered in this work provide model-independent means to explore the presence of LNV physics. If an exotic short-range contribution were to be observed, it would indicate that light neutrino masses have their origin around the TeV scale. It would also have profound consequences on possible explanations of the matter-antimatter asymmetry of the Universe, with the observation of nonstandard neutrinoless double-beta decay contributions disapproving baryogenesis taking place above the electroweak scale [13].

ACKNOWLEDGMENTS

Altay Etkin would like to thank his supervisor Frank F. Deppisch for providing such an opportunity to investigate his research with numerous discussion sessions to ease the authors work, as well as providing a good working atmosphere during the summer period.

The work of Altay Etkin is supported by the University College London's Brian Duff Summer Studentship within the High Energy Physics group. The work of Frank F. Deppisch is supported in part by the UK Science and Technology Facilities Council (STFC) via a Consolidated Grant (Reference ST/P00072X/1).

[1] F. F. Deppisch, L. Graf, F. Iachello, and J. Kotila, Analysis of light neutrino exchange and short-range mechanisms in $0\nu\beta\beta$ decay, Phys. Rev. D **102**, 095016 (2020).

[2] M. Agostini, G. Araujo, A. Bakalyarov, M. Balata, I. Barabanov, L. Baudis, C. Bauer, E. Bellotti, S. Belogurov, A. Bettini, *et al.*, Final results of gerda on the

search for neutrinoless double-β decay, Physical review letters **125**, 252502 (2020).
[3] J. Helo, M. Hirsch, and T. Ota, Long-range contributions to double beta decay revisited, Journal of High Energy Physics **2016**, 1 (2016).
[4] L. Graf, F. F. Deppisch, F. Iachello, and J. Kotila, Short-range neutrinoless double beta decay mechanisms, Phys. Rev. D **98**, 095023 (2018).
[5] F. F. Deppisch, T. E. Gonzalo, S. Patra, N. Sahu, and U. Sarkar, Double beta decay, lepton flavor violation, and collider signatures of left-right symmetric models with spontaneous d-parity breaking, Physical Review D **91**, 015018 (2015).
[6] F. F. Deppisch, C. Hati, S. Patra, P. Pritimita, and U. Sarkar, Neutrinoless double beta decay in left-right symmetric models with a universal seesaw mechanism, Physical Review D **97**, 035005 (2018).
[7] V. Cirigliano, W. Dekens, J. de Vries, M. L. Graesser, and E. Mereghetti, A neutrinoless double beta decay master formula from effective field theory, Journal of High Energy Physics **2018**, 1 (2018).
[8] G. Li, M. J. Ramsey-Musolf, and J. C. Vasquez, Left-right symmetry and leading contributions to neutrinoless double beta decay, Physical Review Letters **126**, 151801 (2021).
[9] F. Šimkovic, G. Pantis, J. Vergados, and A. Faessler, Additional nucleon current contributions to neutrinoless double β decay, Physical Review C **60**, 055502 (1999).
[10] A. Faessler, S. Kovalenko, F. Šimkovic, and J. Schwieger, Dominance of pion exchange in r-parity-violating supersymmetric contributions to neutrinoless double beta decay, Physical review letters **78**, 183 (1997).
[11] G. Prezeau, M. Ramsey-Musolf, and P. Vogel, Neutrinoless double β decay and effective field theory, Physical Review D **68**, 034016 (2003).
[12] T. Peng, M. J. Ramsey-Musolf, and P. Winslow, Tev lepton number violation: From neutrinoless double-β decay to the lhc, Physical Review D **93**, 093002 (2016).
[13] F. F. Deppisch, J. Harz, W.-C. Huang, M. Hirsch, and H. Päs, Falsifying high-scale baryogenesis with neutrinoless double beta decay and lepton flavor violation, Physical Review D **92**, 036005 (2015).